sustainability

MDPI

Article

Simulation-Based Multiobjective Optimization of Timber-Glass Residential Buildings in Severe Cold Regions

Yunsong Han [1,2], Hong Yu [1,2] and Cheng Sun [1,2,*]

1 School of Architecture, Harbin Institute of Technology, Harbin 150001, China; hanyunsong@hit.edu.cn (Y.H.); yuhong_hit@126.com (H.Y.)
2 Heilongjiang Cold Region Architectural Science Key Laboratory, Harbin 150001, China
* Correspondence: suncheng@hit.edu.cn; Tel.: +86-451-86281089

Received: 30 November 2017; Accepted: 14 December 2017; Published: 17 December 2017

Abstract: In the current context of increasing energy demand, timber-glass buildings will become a necessary trend in sustainable architecture in the future. Especially in severe cold zones of China, energy consumption and the visual comfort of residential buildings have attracted wide attention, and there are always trade-offs between multiple objectives. This paper aims to propose a simulation-based multiobjective optimization method to improve the daylighting, energy efficiency, and economic performance of timber-glass buildings in severe cold regions. Timber-glass building form variables have been selected as the decision variables, including building width, roof height, south and north window-to-wall ratio (WWR), window height, and orientation. A simulation-based multiobjective optimization model has been developed to optimize these performance objectives simultaneously. The results show that Daylighting Autonomy (DA) presents negative correlations with Energy Use Intensity (EUI) and total cost. Additionally, with an increase in DA, Useful Daylighting Illuminance (UDI) demonstrates a tendency of primary increase and then decrease. Using this optimization model, four building performances have been improved from the initial generation to the final generation, which proves that simulation-based multiobjective optimization is a promising approach to improve the daylighting, energy efficiency, and economic performances of timber-glass buildings in severe cold regions.

Keywords: timber-glass building; multiobjective optimization; daylighting; energy consumption; total cost; severely cold region

1. Introduction

Energy conservation in the construction industry has a significant impact on building a sustainable society [1]. In particular, residential housing in severely cold zones consumes a large amount of energy due to their high-conductivity materials such as bricks and rammed earth. Statistical data show that the energy consumed by rural residential buildings accounts for about a quarter of the total energy consumption of buildings [2]. Since the construction industry is regarded as one of the primary consumers of resources and producers of a substantial proportion of wastes worldwide [3], high-performance sustainable materials such as timber and bamboo are necessary to replace conventional ones. Renewable materials are especially necessary for rural housing in Northeastern China to sharply reduce energy consumption.

Renewable materials for building façades include bamboo, timber, hemp, straw, lime mortar, wheat thatch, and other renewable products [4], which can be made from natural or synthetic products. Among them, timber is the material most commonly used as a representative sustainable material. Timber shows undisputed environmental friendliness with low energy consumption in the process of becoming a construction material and good thermal transmission properties compared with other construction materials. Moreover, glass, an important part of buildings, possesses its own characteristics of creating an open indoor environment with better daylighting. Therefore, in terms of energy conservation and indoor environment quality, timber and glass have become ideally matched materials for residential buildings in severely cold regions.

Earlier studies have been done on timber and glazing to discuss their impact on energy demand and carbon emissions [5]. In 2012, Leskovar and Premrov proposed that the glazing-to-wall area ratio and the U_{wall}-values have a great influence on the energy demand of prefabricated timber buildings, and that there is an optimal glazing-to-wall area ratio corresponding to the lowest total energy demand [6]. Birchmore et al. discussed the impact of different glazing types on the temperatures of timber-framed houses under various weather conditions, and the results showed that houses with Low-E argon-filled double glazing significantly improved summer-time overheating compared with standard double glazing [7].

The concept of timber-glass buildings was first proposed in Leskovar and Premrov's book in 2013, which discussed the combination of timber and glass in developing an optimal contemporary energy-efficient house with an attractive design [8]. At this stage, related works focused on the structural performance of timber-glass buildings, including thermal stresses [9], racking resistance [10], and seismic responses [11] of the timber-glass components. In recent years, relevant studies of timber-glass buildings have turned to energy consumption, CO_2 emissions, etc. In 2014, Rosliakova analyzed the environmental impact of timber-glass façades and indicated that timber-glass composites produced up to 16 times less CO_2 and consumed four times less primary energy than aluminum façades [12]. In 2015, Premrov and Leskovar analyzed the influence of building shape and glazing-to-wall area ratio on the energy consumption of timber-glass houses under different climate conditions, and concluded that the optimal size of glazing with a 35% glazing-to-wall area ratio placed in the southern façade could lead to the minimum values of energy demand in basically every climate condition and any building shape. The energy demand for the heating and cooling of timber-glass buildings varies greatly in different climatic zones [13].

We found that in previous studies, only one single performance object was considered. However, the improvement of one performance objective is prone to affecting other building performance objectives. For instance, with an increase in window-to-wall ratio, energy consumption increases gradually and visual comfort declines dramatically with high indoor illumination, and so a great deal of contradiction arises. Therefore, multiple performance objectives should be considered simultaneously to improve the daylighting and energy efficiency performance of timber-glass buildings.

Research on multiobjective optimization for public buildings has been relatively comprehensive. In 2015, Negendahl proposed the office building performance optimization design method, considering such factors as building energy use, capital cost, daylight distribution, and indoor thermal environments [14]. In 2017, using school buildings in the cold zones of China as research subjects, Zhang et al. explored the use of simulation-based multiobjective optimization tools to balance multiple objectives, including minimal energy use for heating and lighting, minimal summer discomfort time, and maximal $UDI_{avg100–2000}$ [15]. For residential buildings, performance objectives have not been fully considered and mainly focus on certain aspects. In 2010, Daniel Tuhus-Dubrow adopted the simulation-optimization tool coupled with a genetic algorithm to minimize energy use and lifecycle costs for residential buildings [16]. In 2017, Yassin focused on the energy consumption and daylighting optimization of multi-story residential buildings [17]. It is essential to study the optimization of objectives related to building performance in the designing of timber-glass residential buildings in severely cold regions.

Reasonable use of building daylighting can not only tremendously reduce the energy consumption of artificial lighting, but also help to improve the quality of indoor daylighting environments, assisting occupants maintain physical and mental health, and work efficiently [18]. Due to people's higher demands for their residential buildings, architectural design should be emphasized and mainly focus on users' comfort, including daylighting performance and low energy consumption. However, current timber-glass building designs largely depend on the "trial and error" method. Even though the energy-saving and daylighting performance of timber-glass buildings is often evaluated using simulation tools, designers still seldom consider multiple performance objectives simultaneously when the "trial and error" method cannot provide the designers support for decision-making in energy-efficiency designs. This paper is aimed at proposing a simulation-based multiobjective optimization method to improve the energy efficiency, daylighting, and total cost performance of timber-glass buildings in severely cold zones of China. Additionally, a parametric model has been developed as a decision-making support tool for designing timber-glass building forms.

2. Methods

2.1. Simulation-Based Optimization Workflow

The simulation-based multiobjective optimization method contains such 4 steps: optimization objective determination, decision variable selection, parametric simulation modeling, and multiobjective optimization, as shown in Figure 1. First, the optimization objectives are determined according to climate conditions and function requirements. For severely cold zones, the objectives usually include indexes of energy efficiency, daylighting, and total cost performance. Then, the decision variables are selected in accordance with the determined objectives, and should also cover the possibility of choosing the building form. Following this, a parametric simulation model is used, coupling geometry with material information inputting and editing, which can accurately describe the building form, space, and construction information, and perform building energy consumption, daylighting, and total cost evaluations. Lastly, the multiobjective evolutionary algorithm is used to explore optimal results coupled with the parametric simulation model.

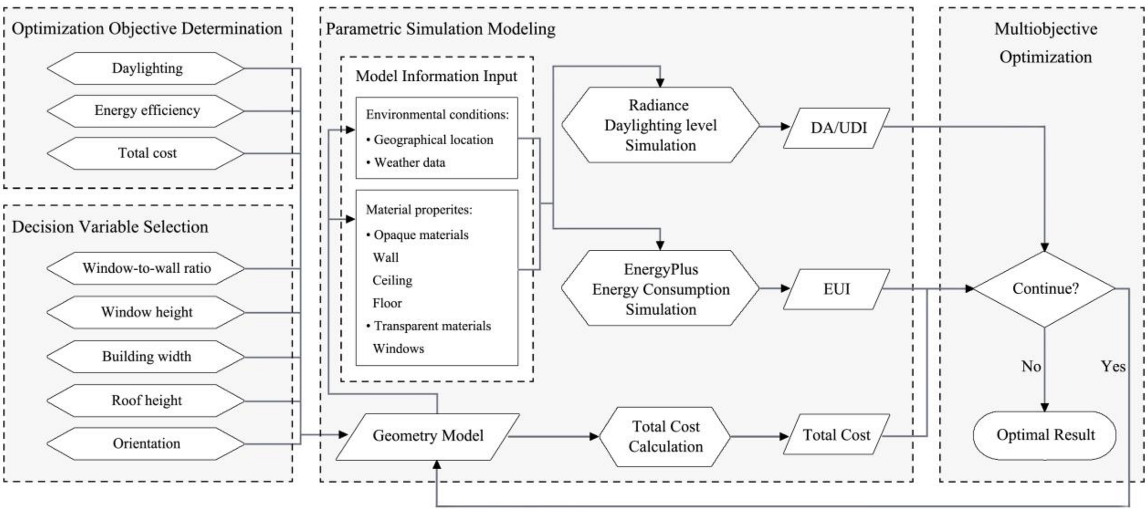

Figure 1. Simulation-based multiobjective optimization process.

During the optimization process, the initial design solutions are generated by evolutionary algorithms and the performances of design solutions are evaluated in the parametric simulation model; the evaluation results are the feedback to the evolutionary algorithm, which supports the generation of design solutions in decision making, and the evolutionary algorithm determines whether the performance of the solutions fits the objectives. If so, the design solutions are the output, and if not, the evolutionary algorithm drives the parametric simulation model to generate new design solutions. After going through a series of iteration optimizations, a Pareto optimal solution set is finally generated. Eventually, the optimal design scheme can be selected from the Pareto solutions according to the preferences of the designers.

2.2. Optimization Objectives

In this study, optimization has been aimed at improving indoor daylighting levels, and reducing building energy consumption, construction, and operation costs, achieving sustainable development of timber-glass buildings. Four objectives have been synthetically considered, namely, daylighting autonomy (DA), useful daylighting illuminance (UDI), energy use intensity (EUI), and total cost.

2.2.1. Daylight Autonomy

The concept of DA was proposed by the Association Suisse des Electriciens in 1989 and was refined by Reinhart and Walkenhorst in 2001 [19]. DA is a climate-based daylighting dynamic evaluation metric, and it is defined as the percentage of the occupied hours of the year during which a minimum illuminance level can be maintained solely by daylight [20]. Lower thresholds of the illuminance levels of residential buildings depends on the Chinese standard of daylighting design for buildings, ranging from 150 lx to 300 lx [21]. In this research, 300 lx is chosen as the lower limit for calculation of DA, that is DA_{300}.

2.2.2. Useful Daylighting Illuminance

UDI, a dynamic daylighting evaluation index, was developed by Nabil and Mardaljevic in 2005, and is defined as the percentage of the occupied hours of the year across the work plane when all illuminance is within 100–2000 lx [22]. Lower and an upper illuminance limit values have been proposed to split the analyzed period into three bins: the lower illuminance value is 100 lx, under which the daylighting level is generally considered insufficient. Then, daylight illuminances higher than 2000 lx are considered to lead to visual discomfort, like glare [23]. Thus, 100–2000 lx has been chosen as the satisfactory range for the daylighting calculation of UDI, that is $UDI_{100–2000}$.

2.2.3. Energy Use Intensity

EUI, an index used to describe energy consumption, is defined as the energy consumed during the year per unit area [24], which is measured in kW h divided by the total floor area of the building (m^2). The lower the EUI values are, the more energy-efficient the building is. In this study, EUI has been applied for energy consumption performance evaluation and serves as a factor for comparison. Due to the extremely low temperatures in winter, heating energy consumption is tremendous in severely cold zones. Air conditioning also consumes energy for cooling in summer. Therefore, as for timber-glass buildings, we should focus on energy consumption not only heating but also for cooling. To better investigate the influence of the decision variables on the annual energy demand of buildings, the total energy consumption for heating and cooling should be taken into account.

2.2.4. Total Cost

In this paper, the total cost is defined as the sum of the cost invested in building materials ($Cost_{materials}$) and the annual cost for building operation ($Cost_{operation}$). The minimum value of the total cost is based on Equation (1). The initial costs of materials ($Cost_{materials}$) (Equation (2)) mainly includes the costs of timber, glazing, and insulation materials, while operational costs consist of artificial lighting, cooling, and heating costs. However, costs for building construction (labor costs), maintenance, and demolition costs are not included in the total costs.

$$\mathrm{Min}_{TC} = \mathrm{Min}\left(\mathrm{Cost}_{materials} + \mathrm{Cost}_{operation}\right) \quad (1)$$

$$\mathrm{Cost}_{materials} = \mathrm{Cost}_{timber} + \mathrm{Cost}_{glazing} + \mathrm{Cost}_{insulation} \quad (2)$$

2.3. Decision Variables and Constraints

The choice of decision variables is essential for the multiobjective optimization of timber-glass buildings in terms of building form, wall construction, roof construction, window type, window area, foundation type, infiltration, shading, and so on [16]. Among them, the building form and windows variables have an especially great influence on building performance. The building form variables generally include building width, the shape coefficient of buildings, etc., while the window variables usually include the window-to-wall ratio (WWR) [17], the glazing type, the window height, and so on.

2.3.1. Building Form Variables

In this present work, there are three variables used to describe building form: building width, roof height, and orientation, as presented in Table 1. For building form variables, the coordinate points of each corner of the timber-glass building are parametrical controlled (X, Y, Z). Among them, some of these coordinate points should be fixed, while others are controlled by parameters. Moreover, another condition involves the original building, which needs to be optimized, particularly the height and plane size of the building. These conditions need to be extracted and analyzed before optimization, which will affect the determination of the constraints. To ensure the rationality of the building form, the floor area has been fixed in the optimization process, which will prevent the situation that the buildings are too narrow to arrange any function.

In this paper, the widths range from 7 m to 16 m, which allows the optimization process to explore more possibilities. Similarly, the values of roof height range from 1 m to 5 m, and the simulation step is 0.1 m. Another form variable is the orientation, which ranges from -60° to 60°, and the simulation step is 1°. This variable concerns the change of direction of the building, which is related to the building energy efficiency and daylight performance.

2.3.2. Window Variables

Since the depth of the buildings is relatively small, no windows are set in the eastern and western parts of the building. The south WWR, north WWR, and window height have been selected as the decision variables to define window form, as shown in Table 1. In the optimization process, the window forms have been generated automatically on the basis of the decision variables. The south WWR and north WWRs respectively control the size of the windows, as does the window height. The WWR and the window height are independent of each other.

According to the building energy efficiency standard [25], the values of south and north WWRs range from 0.10 to 0.45. Based on the values of the WWR, to avoid the windows exceeding the width of the building, the values of window height range from 1.5 m to 3.0 m.

Table 1. The value ranges and the steps of decision variables.

Decision Variables	Unit	Value Ranges	Steps
Width	m	7–16	0.1
Roof height	m	1–5	0.1
South WWR	-	0.10–0.45	0.01
North WWR	-	0.10–0.45	0.01
Window height	m	1.5–3.0	0.1
Orientation	°	−60–60	1

2.4. Parametric Simulation Modeling

The parametric simulation model has been developed to combine the design information and environmental conditions together, and generate the simulation model automatically, which can help the designer generate and modify building forms by changing the input variables without having knowledge of the scripting. Rhinoceros and Grasshopper have been used to develop the parametric simulation model.

Additionally, Archsim and DIVA plug-ins have been used to couple with Grasshopper, EnergyPlus, Radiance, and Daysim. Archsim and EnergyPlus were used to calculate energy consumption, which makes it easier to change the simulation inputs, such as the material and its thickness. DIVA was developed at Harvard University [26] and distributed by Solemma LLC [27], which has been used to carry out a series of daylighting analyses, including climate-based daylighting metrics, annual and individual time step glare analysis, etc. Eventually, Octopus, an evolutionary optimization tool, was used to perform the multiobjective optimization. The tools coupled in the parametric simulation model are presented in Figure 2. The whole simulation-based optimization model is presented in Figure 3.

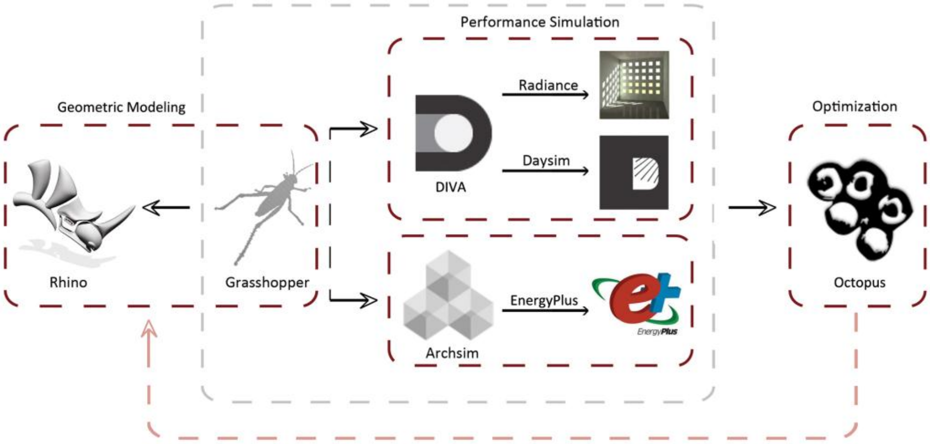

Figure 2. The tools coupled in the parametric simulation model.

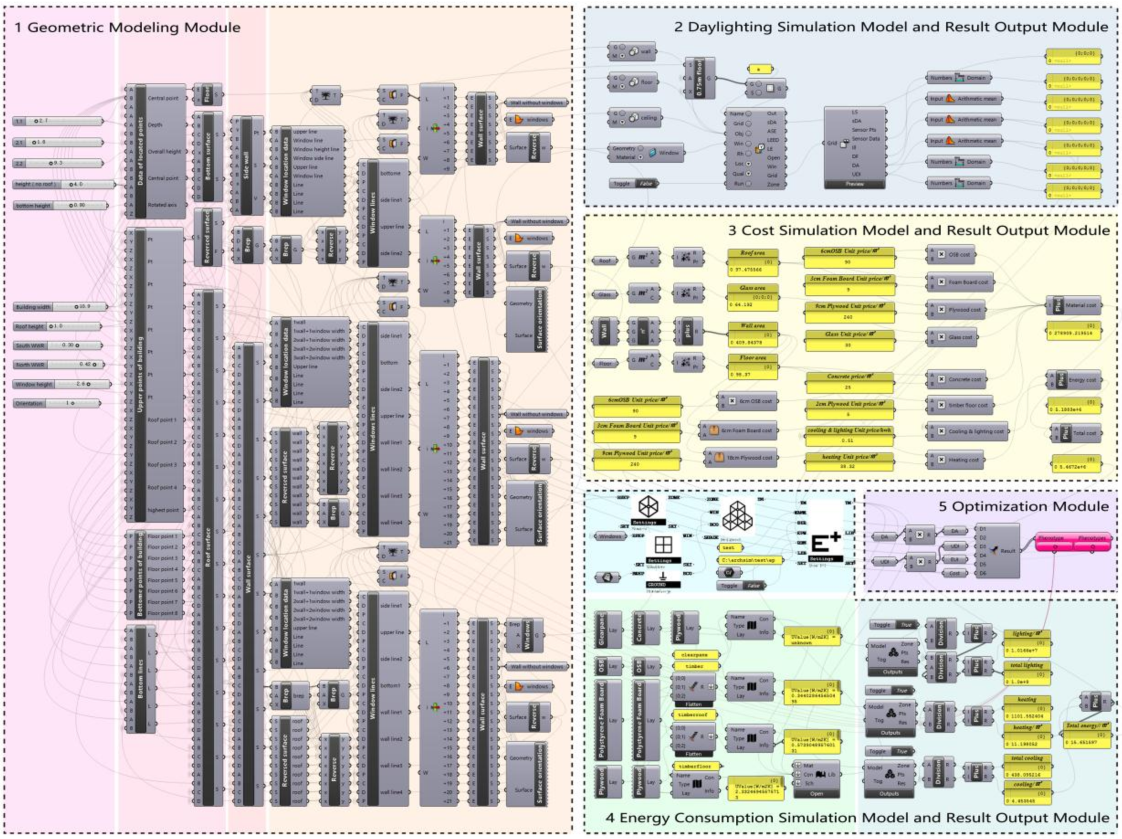

Figure 3. The simulation-based optimization model.

2.4.1. Reference Building

This paper mainly focusses on building performance in severely cold zones, where Harbin (45.77N, 126.68E) was chosen as a representative city. Its location and annual climate data were obtained from the EnergyPlus Weather file (.epw) [28]. In particular, annual direct and scattered radiation values in the file can be imported into the simulation engine for annual daylighting simulation. Historical measurements of ambient temperature, relative humidity, and solar radiation [29] contained in this weather file were used for energy consumption simulation.

A traditional residential building in Harbin was taken as the reference building. The plan of the reference building is a cross shape of two rectangles, whose sizes are 7.2 m × 10.8 m and 8.1 m × 9 m, respectively. The height of the building is 4.8 m, and the roof height is up to 1.8 m. The plan and the initial geometry model of the reference building are reflected in Figure 4.

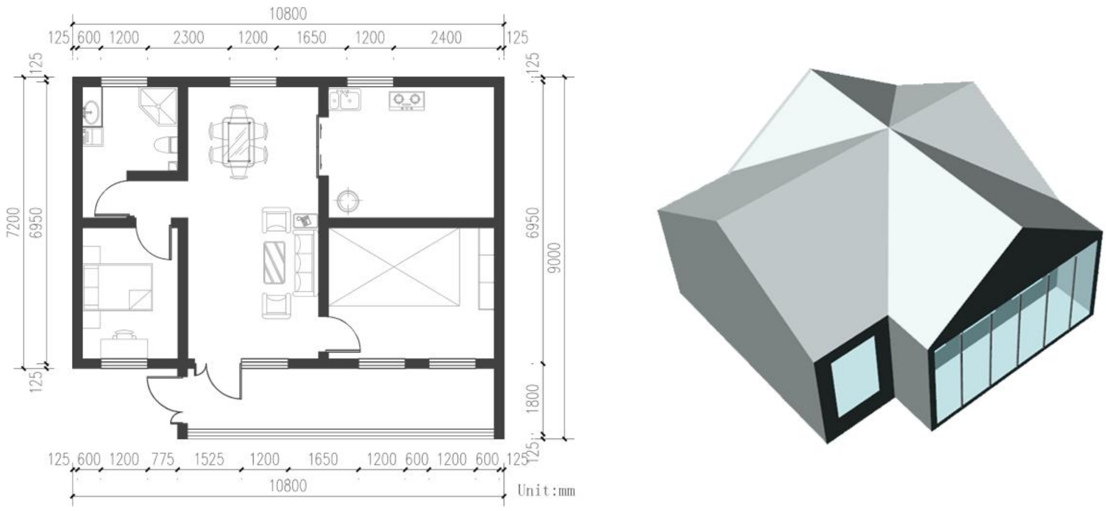

Figure 4. The plan and the geometry model of the reference building.

2.4.2. Simulation Parameter Settings

Before the simulation, the optical and thermal properties were set up, and the simulation parameters were set as the boundary conditions. The reflectance of the opaque materials and transmittance of the glazing materials are indicated in Table 2, and the details of the Radiance parameters of daylighting calculations are manifested in Table 3, which are set to ensure simulation speed and accuracy [19].

Table 2. Settings of the optical properties of the indoor materials.

Indoor Materials	Reflectance	Transmittance
Timber ceiling	0.70	-
Timber floor	0.20	-
Timber interior wall	0.50	-
Double-pane Low-E glazing	-	0.65

Table 3. Settings of the radiance simulation parameters.

-ab	-ad	-as	-aa	-ar
Ambient bounces	Ambient division	Ambient sampling	Ambient accuracy	Ambient resolution
2	512	256	0.15	128

Source: From Dubois [30].

Specific material information, including the thickness, thermal conductivity, density, and specific heat of each layer, and the U-values of different building components, are shown in Table 4. The external timber wall is defined as a 60 mm thick oriented strand board and a 180 mm thick plywood structure insulated with a 60 mm insulation board, with a U-value of 0.344 W/m^{2}k. Similarly, the U-value of the timber roof and floor are 0.574 W/m^{2}k and 2.332 W/m^{2}k, respectively.

Table 4. Material information of the building.

Component	Material	Layer Thickness	Thermal Conductivity [1]	Material Density [1]	Specific Heat [1]	Material Thickness	Material U-Value
Unit	-	mm	W/(m·k)	Kg/m^3	J/(kg·k)	mm	W/m^{2}k
Timber wall	Oriented strand board (OSB)	60	0.147	605.3	2000	300	0.344
	Polystyrene foam board	60	0.042	30	1380		
	Plywood	180	0.200	600	2510		
Timber roof	Oriented strand board (OSB)	60	0.147	605.3	2000	180	0.574
	Polystyrene foam board	30	0.042	30	1380		
	Plywood	90	0.200	600	2510		
Timber floor	Plywood	20	0.200	600	2510	120	2.332
	Concrete	100	0.630	1300	1050		

[1] Data from table <Calculation parameters of thermal physical properties of common building materials> [31].

The heating and cooling set points [32] and the occupancy schedule setting of the building fitted in with the use-time period of residential buildings. Thus, the simulation run period was set from 1 January to 31 December. The internal loads, including people, equipment, lights, and heating and cooling set points are presented in Table 5.

Table 5. Settings of the EnergyPlus simulation parameters.

Loads			Conditioning		
People	People (P/m^2)	0.2	Heating	Set point (°C)	20
Equipment	Equipment (W/m^2)	12		Availability	ResidentialOcc
Lights	Power density (W/m^2)	12	Cooling	Set point (°C)	26
	Dimming	Continuous		Availability	ResidentialOcc

The unit price of the materials during the construction stage were decided according to the market price at that time, and the charges for heating and electricity in the building operation phase were notified by the government, and are listed in Table 6.

Table 6. Settings of unit price parameters.

Stage	Material	Energy Consumption	Thickness	Unit Price		Unit Price	
Unit	-	-	mm	¥/m^2	$/m^2	¥/kW·h	$/kW·h
Building construction	Oriented strand board (OSB)	-	60	90	13.60	-	-
	Polystyrene foam board	-	30	9	1.36	-	-
	Plywood	-	90	240	36.27	-	-
	Double-pane Low-E glazing	-	6	30	4.53	-	-
	Concrete	-	-	25	3.78	-	-
Building operation	-	Cooling and lighting	-	-	-	0.510	0.077
	-	Heating	-	38.32	5.79	-	-

2.5. Multiobjective Optimization

Multiobjective optimization, proposed by Pareto [33], is an approach used to systematically explore various combinations of parameters and make trade-offs or good compromises between multiple objectives; it produces a set of feasible solutions from one extreme trade-off to another [34], including a series of dominated and non-dominated solutions.

In this paper, Octopus, a plug-in for Grasshopper, was applied to perform the multiobjective optimization, and applies evolutionary principles to parametric design and problem solving. Octopus can invoke HypE, which is highly effective in solving multiobjective problems in comparison to existing multiobjective evolutionary algorithms [35]. The termination criterion was based on the tendency of stabilizing the hypervolume of the Pareto front, and the indicator indicated convergence towards the Pareto front as well as the representative distribution of points along the Pareto front [36,37].

The objectives minimized the EUI and total cost, and maximized the DA_{300} and $UDI_{100–2000}$ values. Since Octopus is aimed at searching for the minimal solution, the values of DA_{300} and $UDI_{100–2000}$ needed to be multiplied by -1. Afterwards, when the minimum targets were selected, the absolute values of DA_{300} and $UDI_{100–2000}$ increased instead. The parameter settings of the optimization algorithm are shown in Table 7.

Table 7. Settings of the optimization algorithm.

Elitism	Mutation Probability	Mutation Rate	Crossover Rate	Population Size
0.500	0.100	0.500	0.800	100

3. Results and Discussion

The multiobjective optimization was performed over a period of 2 days. After the calculation of 55 generations, it turned out to be sufficient for convergence. As shown in Figure 5, 11,000 feasible solutions were evaluated, including 141 non-dominated solutions, which formed a Pareto-optimal solution set expressed by a curved surface. In the three-dimension coordinate system, the three axes represent EUI, DA, and UDI, while the fourth dimension, color, represents the total cost of the building. The closer the values of EUI, DA, and UDI are to the origin, the better the objective performance is. The red-colored boxes represent the solutions with maximum values of total cost in the final generation of simulations. The green-colored boxes are the best performing solutions in terms of total cost.

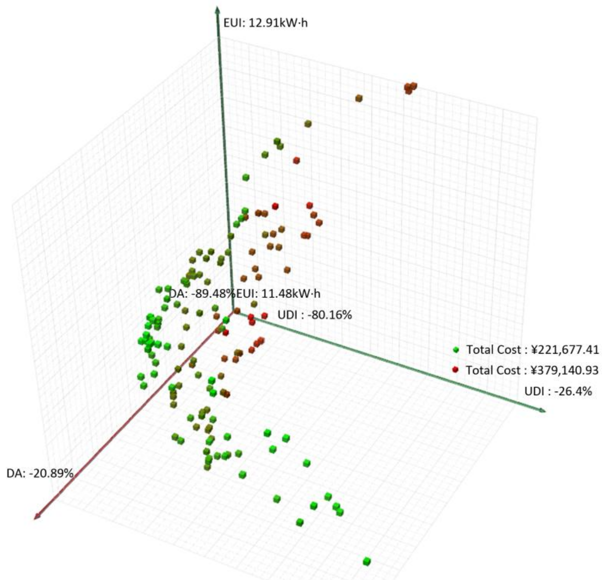

Figure 5. Non-dominated solutions.

3.1. Evolution of the Performance of the Feasible Solutions

As shown in Figure 6, the gray-green colors indicate the feasible solutions and the marked boxes represent the Pareto solutions after 55 generations of simulations. In the 5th generation, the feasible solutions have a wider performance distribution. The value distributions of feasible solutions in the 20th, 40th, and 55th iteration calculations are much closer to the coordinate axes. With a rise in the number of iterations, EUI gradually decreases while DA and UDI increase. This shows that the performance of the feasible solutions improves step by step. Eventually, the non-dominated solutions are mostly located close to the coordinate axes of the optimization objectives.

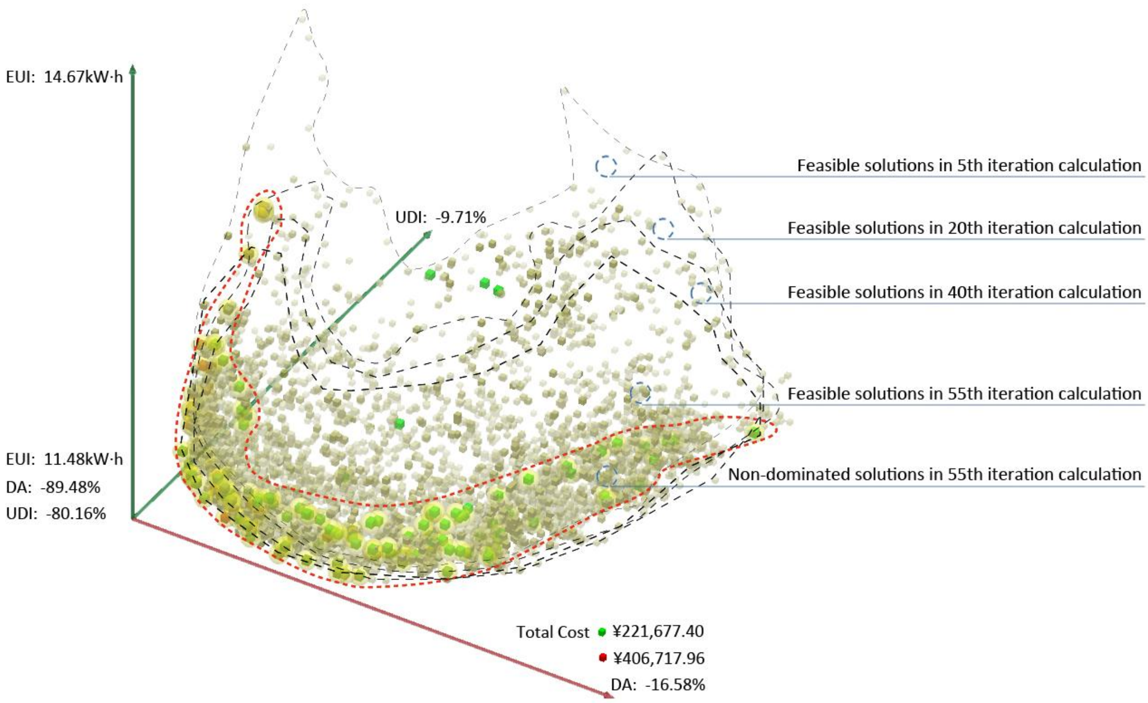

Figure 6. The performance of feasible solutions in different iterations.

Due to their obvious inverse proportional relationship, EUI and DA have been selected as the subjects for study, and the non-dominated solutions obtained in iteration calculations have been extracted and compared. As demonstrated in Figure 7a, the distribution of non-dominated solutions is loose and the non-dominated solutions near the coordinate axes are relatively few. There are many more solutions with lower DA values and higher EUI values. After 20 iteration calculations (Figure 7b), the distribution of non-dominated solutions is relatively intensive and the amount of solutions with great performance increases. This shows that, with an increase in the number of iterations, more and more feasible solutions with relatively better daylighting and lower energy consumption performance have been chosen as non-dominated solutions.

The non-dominated solutions shown in Figure 7c were the results after the 40th iteration calculations, the part of which near the origin apparently increases. The solutions distributed in the front of the curve are more uniform. This indicates that, with the progress of optimization, the daylighting performance and energy consumption gradually improve. Compared with previous generations, the distribution of non-dominated solutions in the final iteration calculation is much more intensive (Figure 7d), and more optional design solutions can be obtained and provided for the designers.

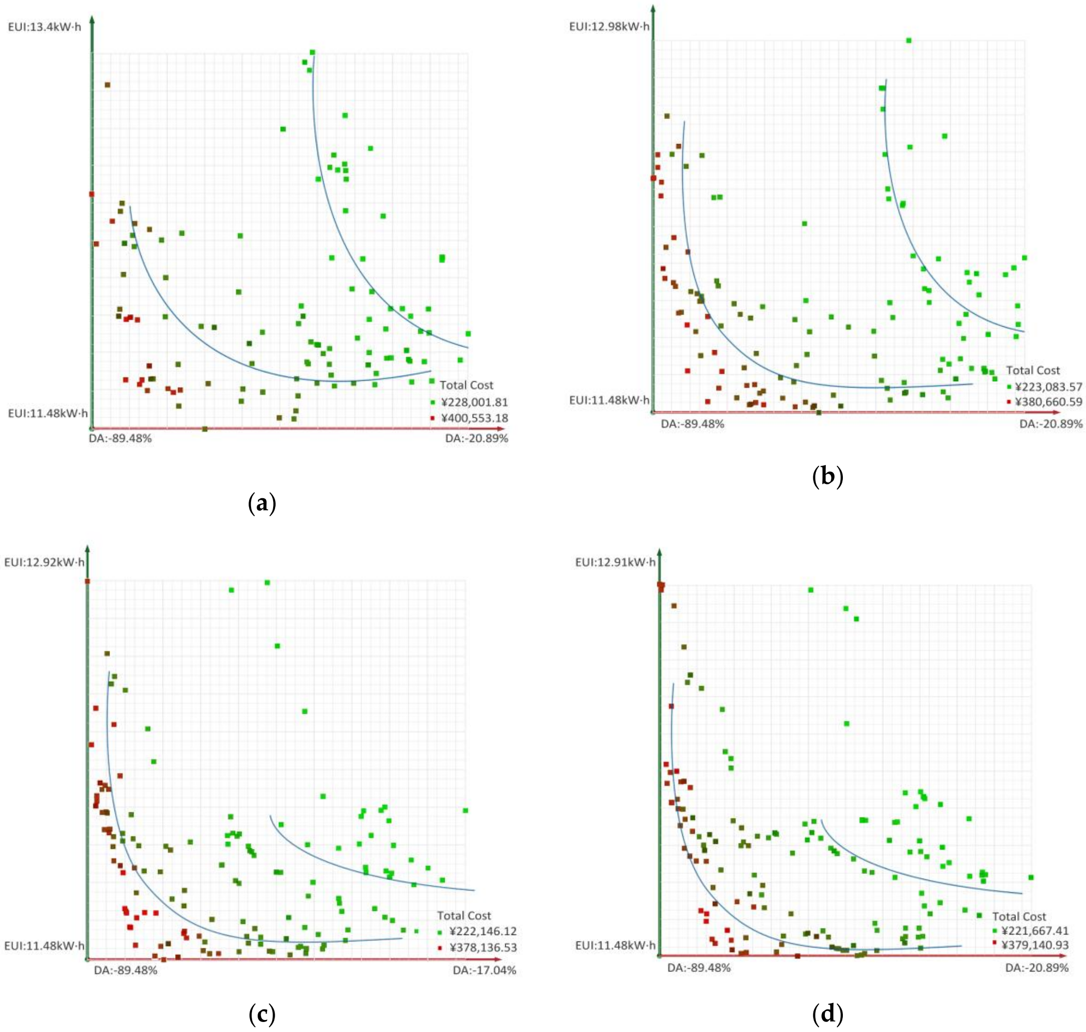

Figure 7. Non-dominated solutions in different iterations: (**a**) non-dominated solutions in the 5th iteration; (**b**) non-dominated solutions in the 20th iteration; (**c**) non-dominated solutions in the 40th iteration; (**d**) non-dominated solutions in the 55th iteration.

3.2. The Correlation between Multiple Objectives

As reflected in Figure 8, with an increase in DA, the overall trend of UDI climbs and then declines. This situation results from the fact that the daylighting evaluation of DA only has a minimum illumination limit. If this value is exceeded, it can be considered as meeting the requirements of the indoor daylighting environment. UDI has upper and minimum illumination limits, and so the UDI index can evaluate the frequency of discomfort or unwanted levels of daylighting for users. Normally, more than 2000 lx is identified as glare due to its high illuminance value, which will lead to a gradual decrease in UDI values. As such, the range of each design variable cannot be determined simply by the DA values in the design. If it is believed that illumination requirements can be guaranteed only considering the DA values, there are definitely likely to be glare problems. Eventually, the daylighting environment will not be improved, but get worse.

With an increase in DA values, the total cost will increase gradually. To increase the DA values, the window area is enlarged, which will lead to an increase in the cost of glazing. At the same time, the building width increases, causing a dramatic rise in the wall area. Thus, the cost spent on the timber materials of exterior wall will climb. Due to the improvement in daylighting performance, the artificial lighting energy consumption decreases, but the energy consumption for air conditioning shows modest rises. Therefore, the increase in energy consumption cost is not obvious. Hence, not only should we consider the DA values, but also think about the total cost caused by the design variables having an impact on the DA performance.

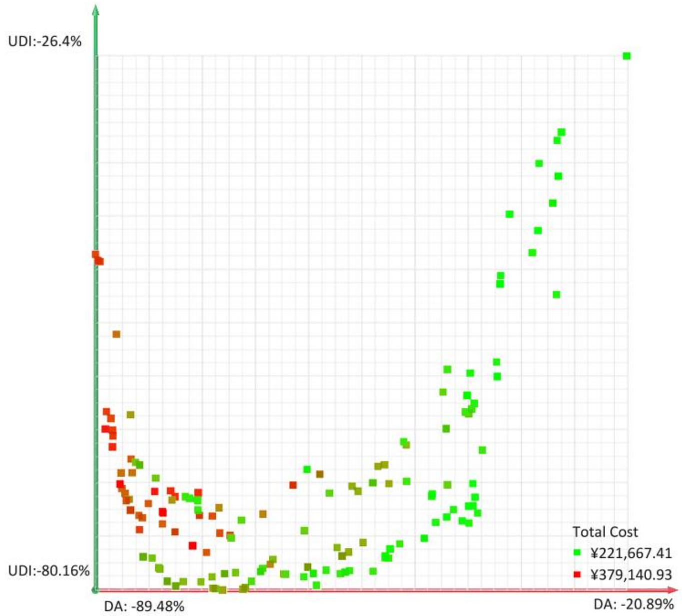

Figure 8. The DA and UDI performance of non-dominated solutions.

Figure 9 presents the non-dominated solutions of EUI and DA, and the colors of the boxes represent the total cost. The performance of DA is negatively correlated with EUI. Large windows improve daylighting performance with high DA values. However, they are also the main cause for the rise of energy consumption for heating and cooling. Therefore, an optimization should consider both DA and EUI.

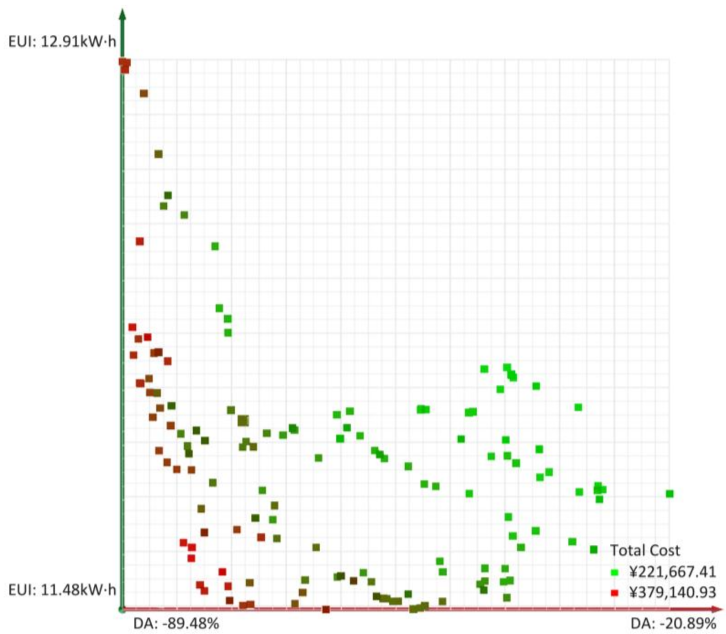

Figure 9. The EUI and DA performance of non-dominated solutions.

The EUI performance also has an impact on the total cost performance, which is not obvious. The increase of WWR will lead to an increase in energy consumption for heating and cooling but a reduction for artificial lighting. The energy consumption for heating and cooling can be compensated for by a decrease in lighting energy consumption, which will lead to a minor change in the total cost.

The correlation between UDI and EUI is presented in Figure 10. As the value of UDI is lower, EUI and total cost both present a tendency of significant polarization. The lower values of EUI are obtained due to a relatively small building width and WWR, while the larger ones are gained because of a rather large building width and shape coefficient. The change in cost is related to the building width and the lower ones correspond to a small width with less timber consumption.

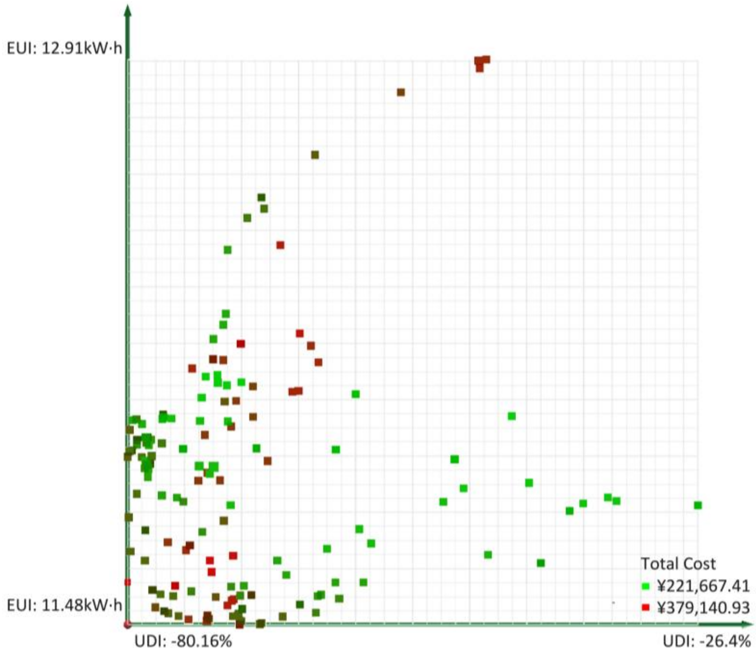

Figure 10. The UDI and EUI performance of non-dominated solutions.

When the value of UDI hits a much higher level, EUI and cost reach much higher values, after which they decline. This is because the WWR is around the maximum value and energy consumption for heating and cooling reaches the maximum for its large glazing area. The costs of glazing materials increase accordingly. Afterwards, UDI is up to an upper value, while the values of EUI and cost decline significantly. Since the maximum value of UDI doesn't correspond to the largest size of windows, the glazing area and energy consumption will decrease instead, as will the cost of glazing.

In conclusion, there is a negative correlation between DA and EUI, and it is the same with the relationship between DA and total cost performance. With an increase in DA, UDI presents a tendency of primary increase and then decrease. As EUI and total cost both show a non-linear relationship with UDI, the relationship between EUI and total cost presents this same tendency. Therefore, it is essential to take all the design objectives into comprehensive consideration rather than consider a certain objective separately. Firstly, it can create a better indoor daylighting environment and avoid glare problems simultaneously. Secondly, reasonable optimization design can effectively reduce building energy consumption and the total cost.

3.3. Value Distribution of Objectives

3.3.1. Daylighting Autonomy

From the numerical distribution of the optimization objectives, the non-dominated solutions of DA ranged from 20.89% to 89.48%. The relative optimum solution of DA was 89.48%, while the worst one was 20.89%, and so there was a gap of 68.59% to the maximum when designers selected the solutions.

The values of DA are closely related to the decision variables. The primary influencing factor for DA performance is the building width, which has a linear relationship with the value of DA, that is to say, with an increase in various variables, the building width achieves obvious improvement in indoor daylighting levels. On the condition of the same building area, the increase in width will directly bring more daylight into the building with windows located in the south and north of the building. Therefore, a reasonable building width parameter should be selected in order to allow more daylight in.

3.3.2. Useful Daylighting Illuminance

The non-dominated solutions of UDI ranged from 26.4% to 80.16%. The relative optimum solution of UDI was 80.16%, while the worst one was 26.4%. Hence, a gap of 59.29% between the optimal and worst performance arose.

The building width is the main factor affecting UDI performance. The main reason why the building width affects UDI heavily is similar to that of the relationship between building width and DA. With an increase in building width, UDI presents a tendency of primary increase and then decrease because an increase in the width can bring more daylight into the building and large illumination over 2000 lx may result in an uncomfortable indoor visual environment with glare problems causing a reduction in UDI. Accordingly, it is better not to choose larger width in design.

3.3.3. Energy Use Intensity

The non-dominated solutions of EUI ranged from 11.48 kW·h to 12.91 kW·h; the relative optimum solution of EUI was 11.48 kW·h, while the worst one was 12.91 kW·h.

North WWR presented a remarkable correlation with EUI performance, which has a linear relationship with the values of EUI. The main reason for this was the area enlargement of glazing with poor thermal insulation performance, which will lead to a great deal of heat loss and this loss would be compensated by heating in winter. Hence, heating energy consumption relatively. As the daylight of northern orientation is relatively stable, a change in the amount of daylight has a relatively small influence on energy consumption for lighting and cooling. Therefore, a minor value of the north WWR can lead to a decrease in energy consumption, mainly heating consumption, achieving a better energy conservation effect.

3.3.4. Total Cost

The non-dominated solutions of total cost ranged from ¥221,677.41 to ¥379,140.93 ($33,497.65 to $57,291.95); the relative optimum solution of total cost was ¥221,677.41 ($33,497.65), while the worst was ¥379,140.93 ($57,291.95). Therefore, there exists a gap of ¥157,463.52 ($23,794.30) between the maximum and minimum values.

Building width is of great relevance to total cost, and is the main influencing factor. An increase in building width leads to an enlargement of the building shape coefficient, causing an increase in timber wall area and material costs. Therefore, in the design, the shape coefficient should be controlled to achieve reasonable costs and energy-saving effects.

Overall, as for the numerical distribution of non-dominated solutions of DA, UDI, EUI, and total cost, DA has the widest range of numerical values, followed by UDI and total cost, while the minimum distribution span was for EUI. This shows that in the process of optimization design, the change of architectural decision variables has an even stronger impact on daylighting performance.

Each performance variable has a major influence in terms of decision variables, especially building width which shows great correlation with DA, UDI, and total cost. Therefore, in the design, the building width and north WWR primary factors, should be taken into consideration according to the optimization objectives in order to achieve better performance.

3.4. Parameters of Solutions

3.4.1. Parameters of the Historical Solutions

The values of building widths corresponding to the non-dominated solutions were distributed in the range of 7.1–15.6 m. The orientations of the buildings ranged from −16° to 57°, and were mainly distributed in the range of 0–10°. The roof heights were mainly 1 m. The minimum height was 1.0 m, while the maximum one was 1.9 m. Window heights ranged from 1.9 m to 2.7 m, which led more daylight into the room. The values of WWR ranged from 0.1 to 0.45 according to the non-dominated solutions. The south WWR mainly fell between 0.22–0.24 and 0.41–0.45, while the north WWR ranged from 0.10–0.14 and 0.30–0.44.

This zone of variables allows more daylight into the buildings and avoids unnecessary glare. Due to the large range of variables, they should be taken into consideration at the same time according to the performance of the objectives.

3.4.2. Optimal Value Distribution

The values of every objective above the average of the value distribution were selected as the optimal value threshold. When the performance of all objectives reached a better condition, the optimal value distribution of the width ranged from 7.7 m to 12.0 m, the orientation of the building lay in the range of 0–9°, and the roof height and the window height were between 1.0 m to 1.5 m and 1.9 m to 2.7 m, respectively (Figure 11). The values of south and north WWRs were different, and the distribution was relatively decentralized. The value distribution of south and north WWR fell in the range of 0.11–0.17, 0.22–0.45 and 0.10–0.14, 0.29–0.44.

When the above variable ranges are selected in design, a better performance of each optimization objective can be effectively guaranteed. The values of DA and UDI reach levels of up to 50%, which can achieve the state of really comfortable daylighting. The values of EUI and total cost at lower levels will effectively achieve energy conservation and reduce the overall cost of construction.

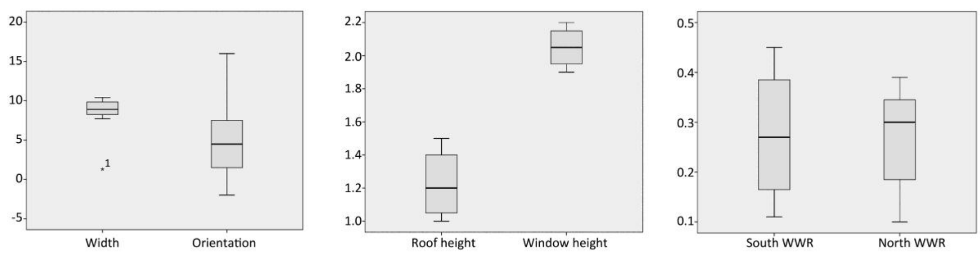

(**a**) (**b**) (**c**)

Figure 11. The value distribution of design variables: (**a**) optimal value distribution of width and orientation; (**b**) optimal value distribution of roof height and window height; (**c**) optimal value distribution of south and north WWR.

3.5. Comparison between Timber-Glass and Origin Buildings

We can see from Table 8 that the reference building features poor building performance with lower DA and UDI values and higher EUI values. A series of optimal solutions was selected from the non-dominated solutions, which obtain better building performance as far as various optimization objectives are concerned. Corresponding design models are shown in Figure 12. A comfortable environment with better indoor daylighting can be created in timber-glass buildings compared with the reference building. The value of DA is doubled and UDI can increase by about 15%. The energy consumption is reduced by up to 18%. Although the total cost has greatly increased, the whole building can effectively achieve energy conservation with timber. In terms of the goals of energy conservation and development of a sustainable society, the cost sacrificed is well worth it.

Table 8. Parameters of the selected non-dominated solutions.

	Width	Roof Height	South WWR	North WWR	Window Height	Orientation	DA	UDI	EUI	Total Cost	
Unit	m	m	-	-	m	°	%	%	kW·h	¥	$
Optimal solution	11.3	1.0	0.42	0.39	2.5	2	71.40	78.38	11.94	283,631.75	42,879.65
	9.8	1.0	0.17	0.10	2.2	9	53.67	69.35	11.52	278,229.54	42,043.87
	8.6	1.0	0.44	0.30	1.9	16	62.18	68.01	11.93	236,425.92	35,726.84
Reference	8.1	1.8	0.32	0.12	1.5	0	33.62	61.13	14.18	100,235.96	15,146.88

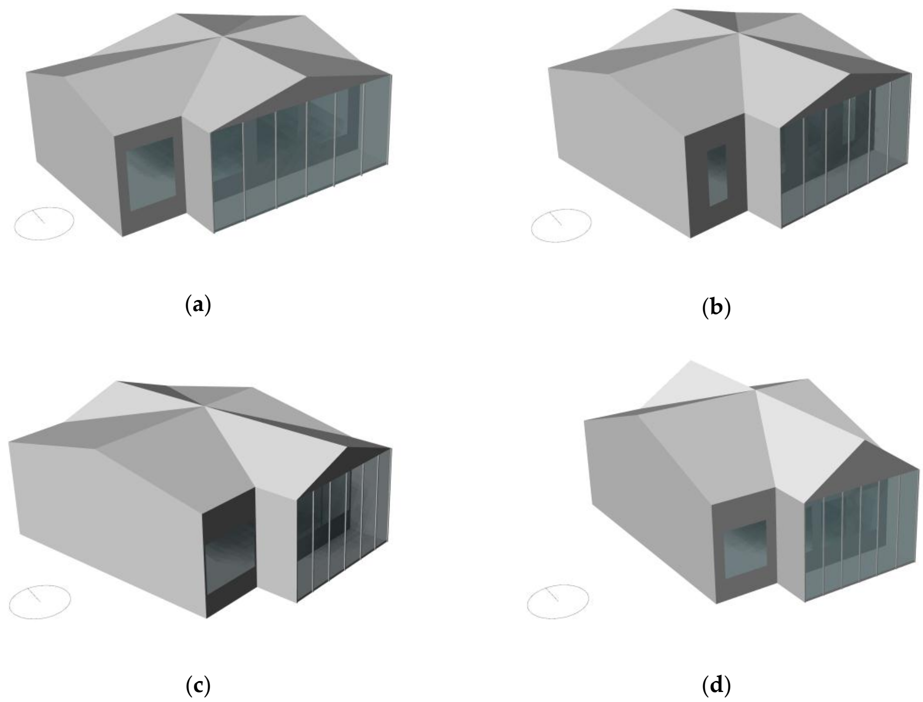

Figure 12. Models of characteristic non-dominated solutions: (**a**) model 1 of an optimal non-dominated solution; (**b**) model 2 of an optimal non-dominated solution; (**c**) model 3 of an optimal non-dominated solution; (**d**) reference model.

4. Conclusions

Architectural design is the essential process of seeking optimal solutions with the consideration of multiple objectives. The multiobjective optimization of a timber-glass building in severely cold regions was performed to improve the DA, UDI, EUI, and total cost performances. After 55 iteration calculations, 141 non-dominated solutions were searched.

The value distribution of the optimization objectives has been discussed. DA had the widest range of numerical values, followed by UDI, total cost, and EUI, which demonstrates that in this case-study, changes in decision variables had an even stronger impact on daylighting performance. Negative correlations existed among daylighting, energy efficiency, and cost performance. Hence, multiple objectives need to be taken into account together to create a comfortable indoor environment with low energy consumption and cost.

The analysis of the value distribution of the decision variables demonstrated that timber-glass buildings need to avoid flat rectangle planning and that the ratio of the width to depth and depth to width should not be greater than 1:1.5. The orientation of the building is better either south or south by east within 10°, the roof height cannot be so high, and the window height is better under three meters. South and north WWRs should be taken into consideration with other variables, which have a relatively extensive distribution. Moreover, building width was the largest influencing factor in terms of decision variables, followed by north WWR.

Through the optimization, four building performances have been improved obviously, which proves that a more comfortable indoor environment with better daylighting performance and lower energy consumption can be realized in timber-glass residential buildings compared with traditional buildings in severely cold zones. The simulation-based multiobjective optimization method proves to be able to efficiently help designers make decisions for timber-glass building design in a rational and systematic way.

During the research, it was difficult to select the optimization objectives and decision variables, and set constraints on the variables, and it took some effort to define the variables. The multiobjective optimization process might require further study into other objective selection to achieve a more comfortable indoor environment.

Acknowledgments: This work was funded by the China National Key R&D Program (Grant No. 2016YFC0700209) and the National Natural Science Foundation of China (Grant No. 51708149), and was also supported by China Postdoctoral Science Foundation funded project (Grant No. 2017M621276) and the Fundamental Research Funds for the Central Universities (Grant No. HIT.NSRIF.201838).

Author Contributions: Yunsong Han, Hong Yu, and Cheng Sun conceived the research, developed the model and analyzed the data. All the authors were engaged in final manuscript preparation and writing.

Conflicts of Interest: The authors declare no conflicts of interest.

References

1. Touloupaki, E.; Theodosiou, T. Optimization of building form to minimize energy consumption through parametric modelling. *Procedia Environ. Sci.* **2017**, *38*, 509–514. [CrossRef]
2. Building Energy Conservation Research Center of Tsinghua University. Analysis on the current situation of building energy consumption in China. In *2017 Annual Reported on China Building Energy Efficiency*, 1st ed.; China Architecture & Building Press: Beijing, China, 2017; pp. 13–14.
3. Dutil, Y.; Rousse, D.; Quesada, G. Sustainable Buildings: An Ever Evolving Target. *Sustainability* **2011**, *3*, 443–464. [CrossRef]
4. Choudhury, I.A. Renewable and Sustainable Materials. In *Reference Module in Materials Science and Materials Engineering*, 1st ed.; Elsevier: Kuala Lumpur, Malaysia, 2016; pp. 1–2.
5. Gustavsson, L.; Sathre, R. Variability in energy and carbon dioxide balances of wood and concrete building materials. *Build. Environ.* **2006**, *41*, 940–951. [CrossRef]
6. Leskovar, V.Z.; Premrov, M. Influence of glazing size on energy efficiency of timber-frame buildings. *Constr. Build. Mater.* **2012**, *30*, 92–99. [CrossRef]
7. Davies, K.; Birchmore, R.; Tait, R. The impacts of high performance glazing on typical light timber framed houses in a New Zealand winter. In Proceedings of the 46th Annual Conference of the Architectural Science Association, Southport, Australia, 14–16 November 2012.
8. Leskovar, V.Z.; Premrov, M. *Energy-Efficient Timber-Glass Houses*, 1st ed.; Green Energy and Technology; Springer: London, UK, 2013.
9. Lundstedt, K. Introduction. In *Thermal Stresses in Load-Bearing Glass-Timber Components*, 1st ed.; Linnæus University: Kalmar, Sweden, 2012; pp. 1–2.
10. Štrukelj, A.; Ber, B.; Premrov, M. Racking resistance of timber-glass wall elements using different types of adhesives. *Constr. Build. Mater.* **2015**, *93*, 130–143. [CrossRef]
11. Ber, B.; Sustersic, I.; Dujic, B. Seismic shaking table testing of glass-timber buildings. In Proceedings of the World Conference of Timber Engineering, Quebec, QC, Canada, 10–14 August 2014.
12. Rosliakova, V. Architectural application and Ecological Impact Studies of Timber-Glass Composites Structures. In Proceedings of the International Conference at Glasstec, Dusseldorf Exhibition Centre, Düsseldorf, Germany, 21–22 October 2014.
13. Premrov, M.; Leskovar, V.Z.; Mihalic, K. Influence of the building shape on the energy performance of timber-glass buildings in different climatic conditions. *Energy* **2015**, *108*, 201–211. [CrossRef]
14. Negendahl, K.; Nielsen, T.R. Building energy optimization in the early design stages: A simplified method. *Energy Build.* **2015**, *105*, 88–99. [CrossRef]

15. Zhang, A.; Bokel, R.; Dobbelsteen, A.V.D. Optimization of thermal and daylight performance of school buildings based on a multi-objective genetic algorithm in the cold climate of China. *Energy Build.* **2017**, *139*, 371–384. [CrossRef]
16. Tuhus-Dubrow, D.; Krarti, M. Genetic-algorithm based approach to optimize building envelope design for residential buildings. *Build. Environ.* **2010**, *45*, 1574–1581. [CrossRef]
17. Yassin, A.A.; Sheta, S.A.; Elwazeer, M.A. Parametric Study on Window-Wall Ratio (WWR) for Day lighting Optimization in Multi-Story Residential Buildings: Case Study of an Apartment Complex in Mansoura City, Egypt. *Int. Adv. Res. J. Sci. Eng. Technol.* **2017**, *4*, 21–32. [CrossRef]
18. Galatioto, A.; Beccali, M. Aspects and issues of daylighting assessment: A review study. *Renew. Sustain. Energy Rev.* **2016**, *66*, 852–860. [CrossRef]
19. Reinhart, C.; Walkenhorst, O. Validation of dynamic RADIANCE-based daylight simulations for a test office with external blinds. *Energy Build.* **2001**, *33*, 683–697. [CrossRef]
20. Carlucci, S.; Causone, F.; Rosa, F.D. A review of indices for assessing visual comfort with a view to their use in optimization processes to support building integrated design. *Renew. Sustain. Energy Rev.* **2015**, *47*, 1016–1033. [CrossRef]
21. GB 50033-2013. *Standard for Daylighting Design of Buildings*; China Architecture & Building Press: Beijing, China, 2013; p. 8.
22. Nabil, A. Useful daylight illuminance: A new paradigm for assessing daylight in buildings. *Light. Res. Technol.* **2005**, *37*, 41–59. [CrossRef]
23. Nabil, A.; Mardaljevic, J. Useful daylight illuminances: A replacement for daylight factors. *Energy Build.* **2006**, *38*, 905–913. [CrossRef]
24. Konis, K.; Gamas, A.; Kensek, K. Passive performance and building form: An optimization framework for early-stage design support. *Sol. Energy* **2016**, *125*, 161–179. [CrossRef]
25. JGJ26-2010. *Design Standard for Energy Efficiency of Residential Buildings in Severe Cold and Cold Zones*; China Achitecture & Building Press: Beijing, China, 2010; p. 5.
26. Mohsenin, M.; Hu, J. Assessing daylight performance in atrium buildings by using Climate Based Daylight Modeling. *Sol. Energy* **2015**, *119*, 553–560. [CrossRef]
27. Solemma LLC. Diva for Rhino. 2014. Available online: http://diva4rhino.com/ (accessed on 28 November 2017).
28. U.S. Department of Energy. Auxiliary Programs. 2017. Available online: https://energyplus.net/ (accessed on 28 November 2017).
29. Ma, J.; Qin, J.; Salsbury, T. Demand reduction in building energy systems based on economic model predictive control. *Chem. Eng. Sci.* **2012**, *67*, 92–100. [CrossRef]
30. Dubois, M.C. *Impact of Shading Devices on Daylight Quality in Offices: Simulations with Radiance*; Lund University: Lund, Sweden, 2001; pp. 141–147.
31. Compiling Group of Common Data Handbook for Architectural Engineering. Building thermal design and conservation. In *Common Data Handbook for HVAC*, 2nd ed.; China Architecture& Building Press: Beijing, China, 2002; pp. 235–239.
32. DB23/1270-2008. *Design Standard for Energy Efficiency of Residential Buildings in Heilongjiang Province*; The Construction Department of Heilongjiang Province: Harbin, China, 2008.
33. Ehrgott, M. Vilfredo Pareto and multi-objective optimization. *Doc. Math.* **2012**, 447–453.
34. Mei, Y.; Tang, K.; Yao, X. Decomposition-Based Memetic Algorithm for Multiobjective Capacitated Arc Routing Problem. *IEEE. Trans. Evol. Comput.* **2011**, *15*, 151–165. [CrossRef]
35. Bade, J.; Zitzler, E. HypE: An algorithm for fast hypervolume-based many-objective optimization. *Evol. Comput.* **2014**, *19*, 45–76. [CrossRef] [PubMed]
36. Beume, N.; Naujoks, B.; Emmerich, M. SMS-EMOA: Multiobjective selection based on dominated hypervolume. *Eur. J. Oper. Res.* **2007**, *181*, 1653–1669. [CrossRef]
37. García-Segura, T.; Yepes, V.; Frangopol, D.M. Multi-objective design of post-tensioned concrete road bridges using artificial neural networks. *Struct. Multidiscip. Optim.* **2017**, *56*, 139–150. [CrossRef]